Article No. jmbi.1999.3446 available online at http://www.idealibrary.com on IDEAL® J. Mol. Biol. (2000) 296, 255–268

JMB

β-Hairpin Stability and Folding: Molecular Dynamics Studies of the First β-hairpin of Tendamistat

Alexandre M. J. J. Bonvin[1]* and Wilfred F. van Gunsteren[2]

[1]*Bijvoet Center for Biomolecular Research, Utrecht University, Padualaan 8, 3584-CH Utrecht, The Netherlands*

[2]*Laboratory of Physical Chemistry, Swiss Federal Institute of Technology Zürich, ETH Zentrum CH-8092, Zürich Switzerland*

**Corresponding author*

The stability and (un)folding of the 19-residue peptide, SCVTLYQSWRYSQADNGCA, corresponding to the first β-hairpin (residues 10 to 28) of the α-amylase inhibitor tendamistat (PDB entry 3AIT) has been studied by molecular dynamics simulations in explicit water under periodic boundary conditions at several temperatures (300 K, 360 K and 400 K), starting from various conformations for simulation lengths, ranging from 10 to 30 ns. Comparison of trajectories of the reduced and oxidized native peptides reveals the importance of the disulphide bridge closing the β-hairpin in maintaining a proper turn conformation, thereby insuring a proper side-chain arrangement of the conserved turn residues. This allows rationalization of the conservation of those cysteine residues among the family of α-amylase inhibitors. High temperature simulations starting from widely different initial configurations (native β-hairpin, α and left-handed helical and extended conformations) begin sampling similar regions of the conformational space within tens of nanoseconds, and both native and non-native β-hairpin conformations are recovered. Transitions between conformational clusters are accompanied by an increase in energy fluctuations, which is consistent with the increase in heat capacity measured experimentally upon protein folding. The folding events observed in the various simulations support a model for β-hairpin formation in which the turn is formed first, followed by hydrogen bond formation closing the hairpin, and subsequent stabilization by side-chain hydrophobic interactions.

Keywords: β-hairpin; tendamistat; molecular dynamics; folding

Introduction

With the continuously increasing amount of available genome information and thereby protein sequences, simulation and prediction methods will need to complement experimental methods such as X-ray crystallography and nuclear magnetic resonance (NMR) spectroscopy for the structural study of proteins (Fisher & Eisenberg, 1999). For this, a proper understanding of protein structure and folding is required. Numerous advances in this direction have been made as illustrated, for example, by successful protein and peptide design or redesign (for reviews, see Blanco *et al*., 1998; Lacroix *et al*., 1999; Reagan, 1999). New insights on the mechanism of protein folding have been obtained from both experimental and theoretical studies (Dobson & Karplus, 1999). Studying small protein fragments or peptides can also lead to a better understanding of protein structure and folding. Among those, β-turns and β-hairpins belong to the small structural elements that have been proposed to act as initiation sites in early protein folding events. Their presence in solution has been demonstrated experimentally for several natural and designed peptide fragments (Blanco *et al*., 1994; Searle *et al*., 1995; de Alba *et al*., 1996, 1999; Sieber & Moe, 1996; Ramirez-Alvarado *et al*., 1996; Kortemme *et al*., 1998; Gellman, 1998). Only recently, however, have the folding dynamics and mechanism of such hairpins been studied experimentally, revealing folding times in the microsecond time-range (6 μs for the β-hairpin from protein G B1) (Muñoz *et al*., 1997). Computer simulations of β-turn forming peptide sequences have shown that such peptides can fold and unfold in the nanosecond time-range (Tobias *et al*., Scully & Hermans, 1994; Demchuk *et al*., 1997) and a number of computational studies have started addressing fea-

Abbreviations used: ASA, solvent-accessible surface area; MD, molecular dynamics; R_g, radius of gyration; SPC, single point charge.

E-mail address of the corresponding author: abonvin@nmr.chem.uu.nl

0022-2836/00/60255–14 $35.00/0

tures of β-hairpin stability and (un)folding (Prévost & Ortmans, 1997; Schaefer *et al.*, 1998; Dinner *et al.*, 1999; Pande & Rokhsar, 1999).

To gain further insight at the atomic level of the folding mechanism of β-hairpins, the 19-residue peptide SCVTLYQSWRYSQADNGCA, corresponding to the first β-hairpin (residues 10 to 28) of the α-amylase inhibitor tendamistat (PDB entry 3AIT) (Billeter *et al.*, 1990), was chosen for this study. Tendamistat is a disulphide-bridged β-sheet protein which follows a rapid two-state folding mechanism without any detectable folding intermediate, as demonstrated from stop-flow fluorescence experiments (Schönbrunner *et al.*, 1997a). Its sequence possesses a strong β-sheet propensity, native-like β-structure being conserved even in trifluoroethanol (Schönbrunner *et al.*, 1996), a solvent known to induce α-helical conformations. Kinetic experiments on mutants of this protein lacking the disulphide-bridges have shown that native-like preformed hairpin structures are present in the unfolded state and could act as initiation sites for folding (Schönbrunner *et al.*, 1997b). In addition, NMR experiments have been performed on peptides of various lengths corresponding to the first β-hairpin of tendamistat (Blanco *et al.*, 1991). A 15-residue sequence (VTLYQSWRYSQADNG) lacking the disulphide bridge has been shown by NMR to adopt turn-like structures in the same region where the β-turn is found in the native protein (Blanco *et al.*, 1991).

Here, we present results on the stability and (un)folding of the 19-residue peptide corresponding to the first β-hairpin of tendamistat. This system is studied by performing molecular dynamics (MD) simulations in explicit water under periodic boundary conditions at several temperatures (300 K, 360 K and 400 K), starting from various conformations (native β-hairpin, α and left-handed helical and extended conformations) (for more details see Computational Methods). The simulation lengths range from 10 to 30 ns. The role of the disulphide bridge in hairpin stability is investigated by simulating both the oxidized (with the disulphide bridge) and reduced forms (lacking the disulphide bridge). Insight into the folding mechanism of β-hairpins is obtained from an analysis of the trajectories.

Results and Discussion

β-hairpin stability at 300 K

Two 15 ns MD simulations at 300 K were used to assess the stability of the β-hairpin within the GROMOS96 force field (Daura *et al.*, 1998b) in the presence and absence of the disulphide bridge. The secondary structure content of the oxidized and reduced peptides as function of time is shown in Figure 1(a) and (b), respectively. Both forms maintain the β-hairpin conformation throughout the 15 ns simulation with β-sheet contents of 43 and 46 % for the oxidized and reduced peptides, respectively (Table 1). The structures remain close to the start-

Table 1. Average energies and structural characteristics of the oxidized and reduced β-hairpins from the MD simulations at 300 and 400 K

	300 K		400 K	
	Oxidized (15 ns)	Reduced (15 ns)	Oxidized (10 ns)	Reduced (15 ns)
A. *Energies (kJ mol^{-1})*				
E_{bonded} (solute)	542(10)	545(11)	691(13)	686(12)
E_{elec1} (solute-solute)	−443(57)	−410(51)	−434(60)	−456(47)
E_{elec2} (solute-solvent)	−1758(113)	−1812(92)	−1563(115)	−1540(91)
E_{elec} ($E_{elec1} + E_{elec2}$)	−2201(60)	−2222(45)	−1997(57)	−1996(48)
E_{vdw1} (solute-solute)	−456(25)	−470(22)	−429(27)	−417(22)
E_{vdw2} (solute-solvent)	−378(20)	−367(21)	−319(15)	−325(15)
E_{vdw} ($E_{vdw1} + E_{vdw2}$)	−834(14)	−837(15)	−748(20)	−742(15)
$E_{non\text{-}bonded}$ ($E_{elec} + E_{vdw}$)	−3035(57)	−3059(45)	−2745(50)	−2739(44)
B. *Solvent-accessible surface area (nm^2)*				
All atoms	18.4(0.9)	18.4(0.7)	18.6(l.1)	19.1(1.0)
Polar atoms	10.4(0.5)	10.5(0.6)	10.5(0.6)	10.9(0.7)
Non-polar atoms	8.0(0.7)	7.9(0.5)	8.1(0.7)	8.2(0.6)
Backbone	3.7(0.4)	3.2(0.5)	3.5(0.5)	3.6(0.4)
Side-chains	14.7(0.7)	15.2(0.6)	15.1(0.8)	15.5(0.9)
$R_{gyration}$ (backbone) (nm)	0.71(0.05)	0.71(0.08)	0.65(0.09)	0.74(0.04)
Number of hydrogen bonds	11.0(1.8)	11.9(2.6)	9.0(2.5)	10.2(2.4)
β-sheet (%)	43	46	11	32
β-bridge (%)	2	3	8	3
β-turn (%)	3	10	11	13
Bend (%)	16	10	27	9

Energy averages and standard deviations (between parentheses) were calculated from 10 or 15 ns MD trajectories using 20 ps block averages.

The solvent-accessible surface areas were calculated with the program NACCESS (Hubbard & Thornton, 1993), using a 0.14 nm radius probe. Secondary structure content and hydrogen bonds calculated using the SECSTR module of the program PROCHECK (Laskowski *et al.*, 1993).

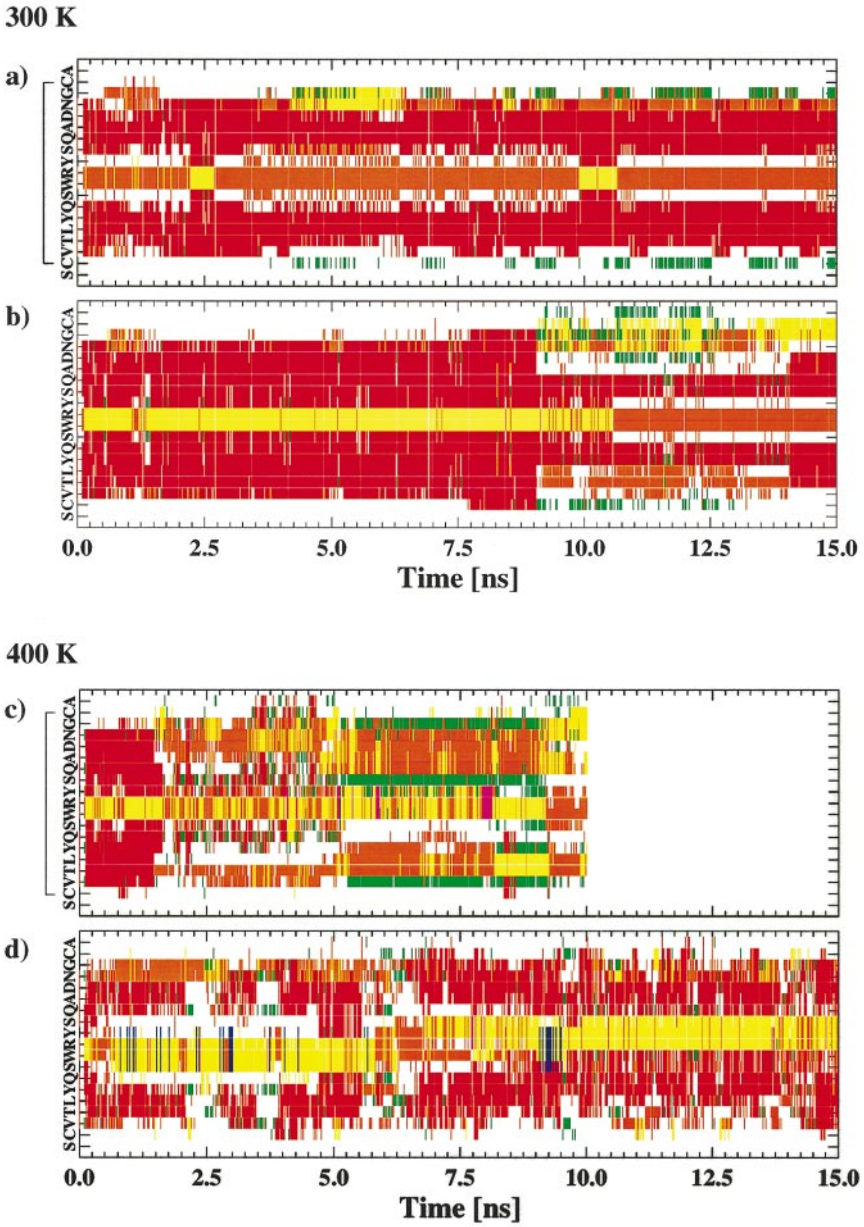

Figure 1. Secondary structure as function of time for the 300 K (upper panel) and 400 K (lower panel) molecular dynamics simulations in water of the (a), (c) oxidized (with disulphide bridge) and (b), (d) reduced first β-hairpin (residues 10-28) of the protein tendamistat (Billeter *et al.*, 1990). Red, β-sheet; yellow, hydrogen-bonded turn; orange; bend; green; β-bridge; blue; α-helix; violet; 3_{10}-helix.

ing structure with positional root-mean-square (rms) deviations for backbone atoms of the central eight residues (YQSWRYSQ) of 0.12(±0.02) nm and 0.11(±0.03) nm, for the oxidized and reduced peptides, respectively. In both simulations, the hairpin remains centred around the Trp9-Arg10 pair. However, different turn conformations and hydrogen-bonding patterns are observed and can best be described in the β-hairpin terminology reported by Sibanda & Thornton (1985) in which the hairpin type is defined by the conformation of the four turn residues (L1 to L4). In the oxidized form (Figure 1(a)), a type I β-turn at the Trp9-Arg10 position (L2,L3) is present throughout the 15 ns trajectory. A total of three hairpin conformations with a type I β-turn are sampled during the simulation that differ by the hydrogen-bonding pattern of the adjacent residues (Ser8 (L1) and Tyr11 (L4)): a 4:4 β-hairpin (no hydrogen bond between L1 and L4) populated for approximately 60 % of the time, a 2:4 β-hairpin (one hydrogen bond between L1 and L4) populated for approximately 30 % of the time, and a 2:2 β-hairpin (two hydrogen bonds between L1 and L4) populated for approximately 10 % of the time. The 2:2 β-hairpin can easily be recognized from the secondary structure plots in Figure 1(a) by its tight turn (e.g. around 2.5 and 10 ns). The 2:4 and 4:4 β-hairpin conformations

with type I β-turn are also found in the reduced peptide simulation, mostly during the last 4.5 ns (Figure 1(b)). Another stable hairpin form, a 2:2 β-hairpin with type II′ β-turn, which was not found in the presence of the disulphide bridge, dominates the first 10 ns of this simulation. Type I and type II′ turns differ in their ϕ,ψ dihedral angles of the L2 residue (Trp9 in this case): −60°, −30° for a type I turn and 60°, −120° for a type II′ turn. The disulphide bridge prevents the formation of the type II′ β-turn, thereby preserving the type I β-turn conformation. This could have a functional importance and explain the conservation of the four-turn residues (Ser-Trp-Arg-Tyr) and of the two cysteine residues among the family of α-amylase inhibitors. Further analysis of Figure 1(b), reveals that the reduced system starts loosing β-sheet content after 9 ns, with turn and bend conformations appearing in the C and N-terminal parts. This was first interpreted as a possible step toward unfolding and was the reason why the simulation was extended to 15 ns. A four-residue antiparallel β-sheet was, however, recovered after 13 ns. Apart from their conformational differences, the oxidized and reduced peptides cannot be distinguished by their energies, solvent-accessible surface area, radius of gyration or hydrogen-bonding properties, as can be seen from Table 1.

β-hairpin unfolding at 400 K

The unfolding of the oxidized and reduced peptides was followed from two 400 K MD simulations of 10 and 15 ns lengths, respectively. The secondary structure content, as a function of time, for those two simulations is presented in Figure 1(c) and (d). Surprisingly, while in the presence of the disulphide bridge β-hairpin conformation is lost after approximately 2 ns, in the reduced peptide (lacking the disulphide bridge) various β-hairpin conformations that differ from the native are found throughout the 15 ns simulation (Figure 2). This is reflected in the β-sheet content at 400 K in Table 1: 11 % for the oxidized peptide against 32 % for the reduced peptide.

For the oxidized system, although the antiparallel β-sheet is almost completely lost after 2 ns, the turn conformation (eight central residues) remains close to the starting conformation, with average backbone atom positional rms deviations from the starting structure of 0.11(±0.03) nm up to 4 ns. This is similar to that observed in the 300 K simulation (see above); the two residues adjacent to the four turn residues are still hydrogen bonded as indicated by the presence of β-bridges (shown in green in Figure 1(c)). Only after approximately 5 ns is the hairpin structure completely lost (aver-

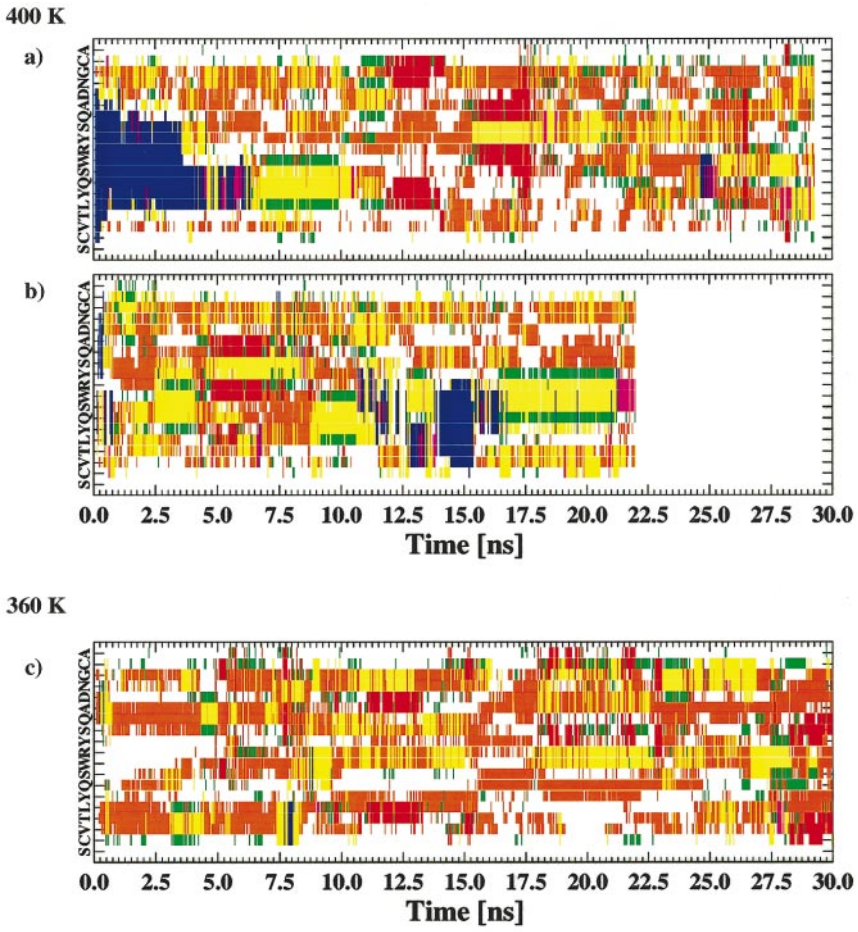

Figure 2. Secondary structure as function of time for the 400 K (upper panel) and 360 K (lower panel) molecular dynamics simulations in water of the reduced polypeptide consisting of the first β-hairpin amino acid sequence (residues 10-28) of the protein tendamistat (Billeter *et al.*, 1990) starting from: (a) An α-helical conformation; (b) A left-handed helical conformation; and (c) An extended conformation. See the legend to Figure 1 for the colour scheme.

age positional rmsd from starting structure 0.19(±0.05) nm). This can also be seen from the snapshots at 5 and 10 ns in Figure 3.

In the absence of the disulphide bridge (Figure 1(d)), the β-hairpin conformation changes within the first 0.5 ns, to a 3:5 hairpin with a type I β-turn at Ser8-Trp9, resulting in a one-residue shift toward the N terminus. This conformation is maintained up to approximately 5.5 ns, although with structural fluctuations: the antiparallel β-sheet is completely lost and reformed twice with transient α-helical conformations (indicated in blue) appearing in the turn region. At around 5.75 ns, the 3:5 hairpin is lost and a three-residue shift toward the C terminus occurs in the turn, resulting in a 3:3 β-hairpin with a type II′ β-turn at Tyr11-Ser12 and a β-bulge at Ser8. This conformation, whose turn is shifted by two residues toward the C terminus compared to the native conformation, is stable for the remainder of the simulation up to 15 ns, with some variations in the β-sheet length. The 3:3 β-hairpin is well defined with a backbone atom positional rms deviation from the mean structure (10-15 ns) of 0.07(±0.02) nm, while the rms deviation from the native conformation amounts to 0.28(±0.02) nm. This is also clearly illustrated in the pairwise backbone atom positional rms deviation matrix plot in Figure 4, revealing three main clusters: the 3:5 β-hairpin (up to 5.5 ns), a transition structure (6-8 ns) and the 3:3 β-hairpin (8.5-15 ns). Snapshots of the two hairpin forms at 5 ns and 10 ns are shown in Figure 3.

What could account for the difference in stability of the reduced and oxidized peptides? Averages for various energy terms are listed in Table 1; no significant difference in energy can explain the increased stability of the reduced form. Clearly, enthalpic considerations cannot explain the stability difference. The energies calculated from the MD simulations only report on the enthalpy of the system. Entropic effects could contribute to the stabilization of the reduced form: this term, lacking the disulphide bridge, is configurationally less restricted than the oxidized form and is therefore likely to possess a larger entropy. The entropy difference between the two forms could thus be. an explanation for their different stabilities. Of course, even with such long simulations, only a limited part of conformational space is being sampled, which can still not properly report on the entropy

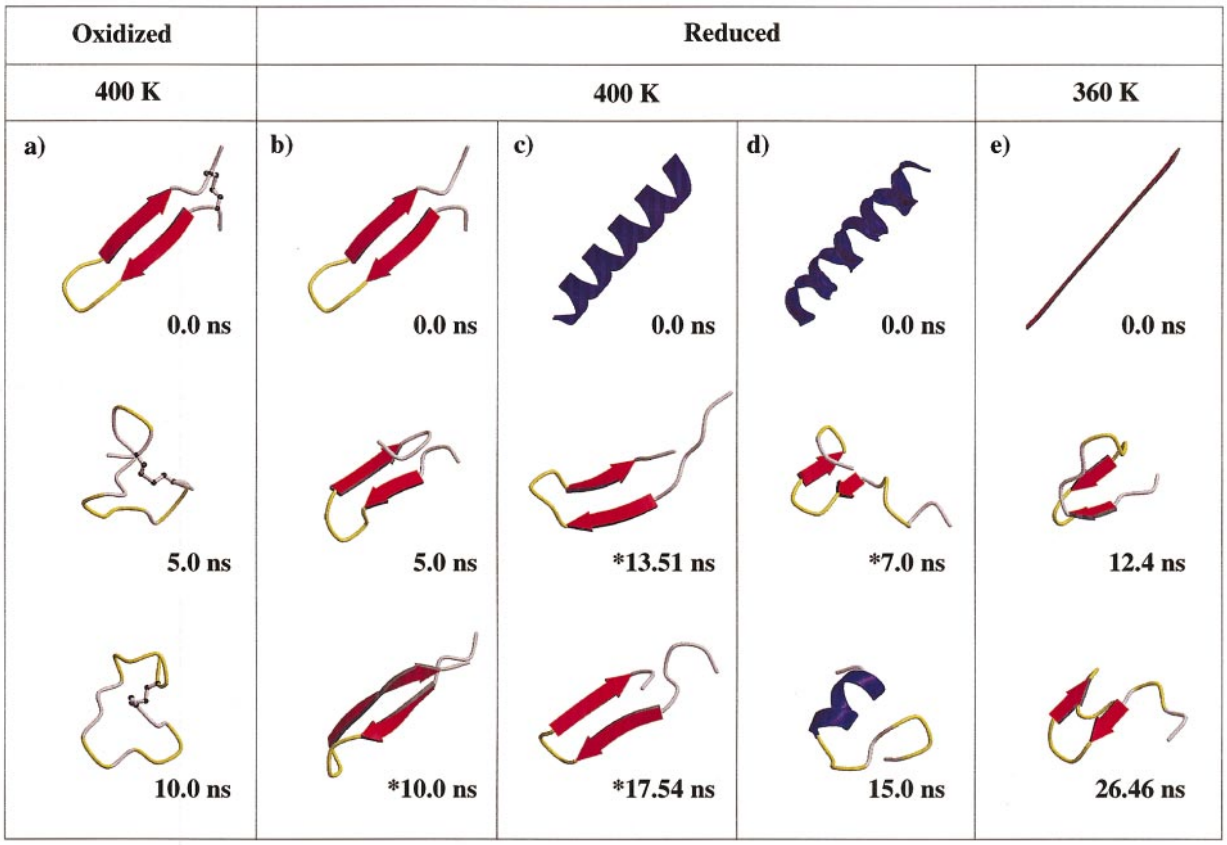

Figure 3. Snapshots of the peptide structures during the 400 K and 360 K MD simulations in water starting from: (a) The oxidized native β-hairpin; (b) The reduced native β-hairpin; (c) α- (d) Left-handed helical conformations, and (e) From an extended conformation. The * indicate β-hairpins shifted by two residues (compared to native) toward the C terminus that are centred around Tyr-Ser (the native β-hairpin is centred around Trp-Arg). β-sheets are coloured red, α-helices blue and hydrogen-bonded turns and bends yellow. The Figure was generated with the programs MOLSCRIPT and Raster3D (Kraulis, 1991; Merritt & Murphy, 1994).

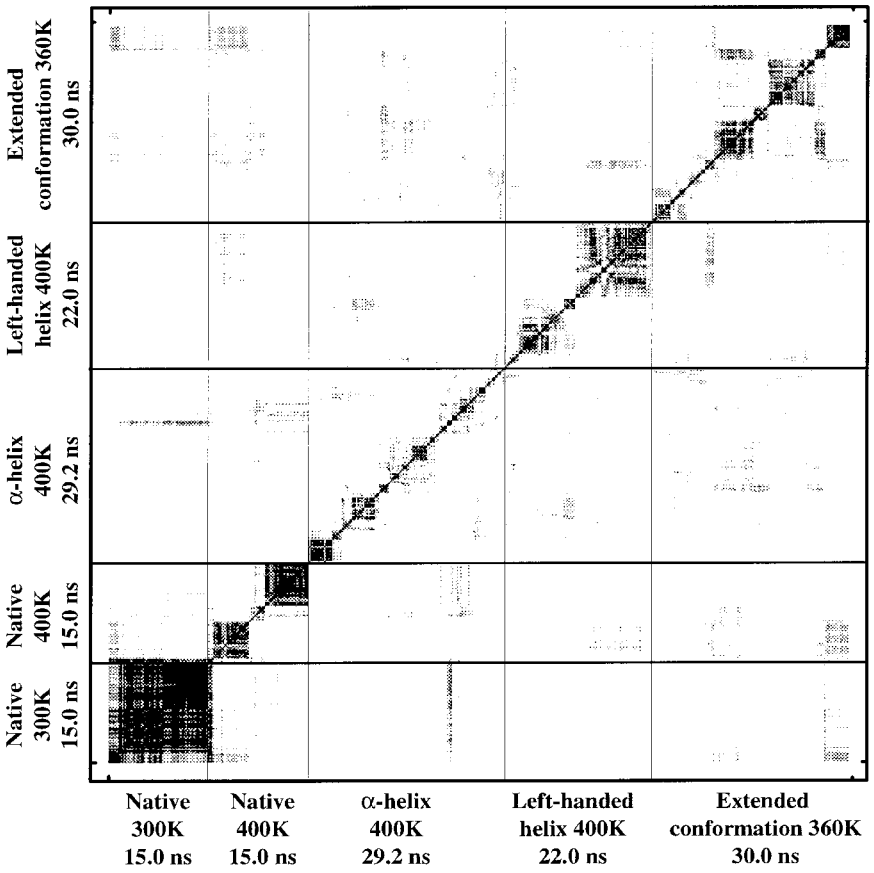

Figure 4. Pairwise atom-positional root mean square deviation matrix calculated from conformations taken at 0.2 ns intervals from all reduced peptide MD simulations. The rms deviations were calculated for the N, $C^{\alpha}$and C-atoms of the central eight residues (YQSWRYSQ) corresponding to the native β-hairpin. The rms deviations are rendered in a gray scale ranging from black (rmsd $\leqslant$ 0.075 nm) to white (rmsd $\geqslant$ 0.175 nm). The simulation temperatures, starting conformations and simulation lengths are indicated on both time axes.

of the various species. More likely, the two-residue shift in the β-hairpin structure occurring after about 6 ns in the reduced form allows the system to find a more stable conformation, as indicated by the higher β-sheet content of 37% for the last 5 ns of the simulation, against 25% for the first 5 ns. The disulphide bridge in the oxidized form preempts such a register shift in the hairpin. The occurrence of a shifted turn conformation in the reduced species is consistent with NMR studies of shorter fragments of this β-hairpin lacking the two cysteine residues (Blanco *et al.*, 1991): amide shift/temperature coefficients indicate the presence of two turn conformations in solution (see Figure 4 by Blanco *et al.*, 1991), at Trp-Arg corresponding to the native turn position, and at Tyr-Ser, the two-residue shifted turn observed in our simulation. The disulphide bridge found in the native peptide thus seems to have a doubly important functional role: preventing the occurrence of the shifted turn, as observed in our 400 K simulations, and keeping the type I β-turn conformation at Trp9-Arg10, and thus a proper side-chain arrangement, as observed in the 300 K simulations. This allows rationalization of the conservation of those cysteine residues among α-amylase inhibitors.

Folding simulations starting from helical conformations at 400 K

Considering the surprisingly high degree of stability of β-hairpin conformations for this particular sequence and to investigate whether or not this is due to the choice of the starting structure, MD simulations at 400 K starting from α and left-handed helix conformations were carried out for 29.5 and 22 ns, respectively. The starting conformations were built in their respective helical conformation. The left-handed helix is a very unlikely conformation in which all ϕ,ψ angles lie in the small allowed region in the upper right quadrant of the Ramachandran plot (Ramachandran *et al.*, 1963). Results in terms of secondary structure as a function of time are presented in Figure 2(a) and (b). Both helical conformations are unstable, and transient β-hairpin conformations are formed.

The α-helical conformation required 7 ns to completely unfold. The unfolding occurred one helical turn at the time, the C and N-terminal turns being

lost within the first 0.5 ns of the simulation and the remaining two turns requiring each about 3.5 ns to unfold. After that, no significant helical conformation was recovered except for one helical turn at the YQSW sequence which was present for approximately 0.5 ns around 25 ns. After the disappearance of the helical conformation (after 7 ns), the system started sampling a number of β-hairpin like conformations, some of which had only one residue in extended conformation on each side of the turn, as indicated by the presence of β-bridges (green in Figure 2), for example between 7 and 10 ns. Two antiparallel β-sheets, both centred around Tyr11-Ser12, were formed during the simulation, each being stable for more than 2 ns. The first was formed after 12 ns and resembles a 3:5 β-hairpin, although the residues adjacent to the bend are, for a major part of the time, not recognized as part of the sheet structure. The second antiparallel β-sheet occurred after 15 ns, this time forming a well-defined 2:2 β-hairpin with a type II′ β-turn at Tyr11-Ser12. This turn conformation is similar to that found in the 400 K simulation starting from the native reduced conformation (Figure 1(d)). This corresponds again to a two-residue-shift toward the C terminus compared to the native turn and is consistent with the second turn population observed by NMR from amide/shift temperature coefficients (Blanco *et al.*, 1991). Snapshots of the two main β-hairpin conformations sampled in this simulation are shown in Figure 3. After the disappearance of the second β-hairpin (after ~18 ns), the system started sampling conformations close to those observed in the 400 K (oxidized) simulation starting from the native form (two-residue C-terminal-shifted 3:3 β-hairpin). This is indicated by the presence of cross-peaks between native and α-helix 400 K simulations in the rmsd matrix (Figure 4). Around 21 ns, conformations occur for 0.5 ns that come as close as 0.1 nm backbone atom positional rmsd for the central eight residues from the 300 K native simulation (intense cross-peaks between 300 K native and 400 K α-helix in Figure 4). Starting from a completely different conformation, this system is thus sampling regions of conformational space that overlap with regions sampled in the simulation starting from the native β-hairpin structure.

When starting from the left-handed helix, the system rapidly looses its helical conformation within the first nanosecond, and samples β-turn, β-bridge, β-hairpin and even α-helical conformations. After 5 ns a 2:2 β-hairpin with type II′ β-turn at Tyr11-Ser12 is formed which remains stable for about 3 ns. This conformation is within 0.02 nm backbone (WRYSQA) atom positional rmsd from the 2:2 β-hairpin found in the α-helix simulation (see above). This is not evident from the rmsd matrix in Figure 4 because there the rms deviations were calculated for the backbone of the YQSWRYSQ sequence (the native β-hairpin). Again, in this system the sampled conformational space shows overlap with the previous simulations: short hairpins formed by a three-residue turn and one β-bridge are found around 10.0 ns and between 16.5 and 21.0 ns, which resemble those present in the 400 K simulations starting from the α-helix (7.0-10.0 ns) and the native (0.5-5.5 ns) structures, as confirmed by cross-peaks in the rmsd matrix shown in Figure 4. Some α-helical conformations are also observed, extending up to two helical turns for a 1.5 ns period (13.8-15.3 ns). These are formed in the region which unfolded last in the 400 K simulation starting from an α-helix. The observation of helical structure formation, although to a much lesser extent than β-hairpin formation, makes us confident that the β-hairpin ''folding'' observed in these simulations is not the result of a force field bias toward extended or hairpin-like structures, but rather an intrinsic property of this particular sequence.

Folding from an extended conformation at 360 K

Although various β-hairpin conformations were recovered when starting from helical conformations, these were only stable for limited periods of time (up to approximately 3 ns) at 400 K. In order to perhaps increase the stability of the folded species and remove any bias toward helical or hairpin conformations, a 360 K simulation starting from a completely extended conformation was run for 30 ns. This system required approximately three times more water molecules than the previous systems, considerably slowing down the computations. Fortunately, fast collapse towards a more compact conformation occurred within the first nanosecond of the simulation, after which the number of water molecules was reduced to the same amount as in the previous simulations (see Computational Methods). The backbone radius of gyration decreased from 2.0 nm for the extended conformation to values of around 0.7 nm, which are typical for the simulations starting from the native conformation (see Table 1). The chain collapse seems to be driven by hydrophobic effects as indicated by the presence of the aromatic residues in the centre of the collapsed conformations. For example, at 1 ns, an almost cyclic conformation with the Trp side-chain buried in the middle is present. This is in contrast to the native conformation in which the Trp side-chain is part of the type I β-turn and is partially exposed to the solvent. While hydrophobic collapse has often been advanced to be the driving force for protein folding, in this case it works against it, since the initial collapsed conformation needs to be ''turned inside-out'' in order to recover native-like conformations. This observation is in line with theoretical studies revealing that the formation of non-native clusters leading to a collapse in the initial phase of folding can lead to kinetic traps slowing down the overall folding rate (Gutin *et al.* 1995; Dinner *et al.*, 1996; Mirny *et al.*, 1996; Shakhnovich, 1997; Chan & Dill, 1998; Pande *et al.*, 1998; Socci *et al.*, 1998; Thirumalai & Klimov,

1999). After only approximately 8 ns, turn conformations around Trp9 start to occur (Figure 2(c)). What looks like a loose hairpin conformation centred around Trp9-Arg10 between 11 and 13 ns is in fact a parallel β-sheet which does not resemble the native hairpin (see the snapshot in Figure 3). Native-like β-hairpin conformations with a type I β-turn at Trp9-Arg10 are sampled around 8 ns for a very limited time period and from 26 ns, where the system comes as close as 0.09 nm backbone atom positional rmsd from the native conformation for the central eight β-hairpin residues. This is indicated by cross-peaks. between the extended 360 K and the native 300 K conformations in the rmsd matrix shown in Figure 4. A snapshot of a native-like conformation at 26.46 ns is shown in Figure 3. Again, the conformational space sampled in this simulation has overlap with all previously described simulations (Figure 4). Although these simulations are still not long enough to achieve an equilibrium between folded and unfolded species, as was the case in the β-peptide simulations described by Daura *et al*. (1998a), the observed overlap in the sampled conformational space between simulations starting from widely different conformations is a very promising result. This indicates that, as observed in the case of a β-peptide (Daura *et al*., 1999), only a limited portion of the available conformational space is populated, thereby greatly reducing the search problem.

Mechanism of β-hairpin formation

Two main mechanisms have been proposed for β-hairpin formation. In the so-called zip-up model of Muñoz *et al*. (1997, 1998), the turn appears first, followed by hydrogen bond formation closing the hairpin, which is finally stabilized by hydrophobic contacts. Another mechanism in which the formation of a hydrophobic cluster precedes hydrogen bond formation has been proposed from simulation studies of the C-terminal β-hairpin of protein G (Pande & Rokhsar, 1999; Dinner *et al*., 1999). Here, the various simulations provide a number of β-hairpin formation events, allowing an analysis of their mechanism of formation. In the 400 K α-helix simulation, the appearance of the first 3:5 β-hairpin at 12 ns is preceded by hydrogen bond formation at the ends of the β-hairpin (β-bridges between 11 and 12 ns), between Leu5 and Cys18. Folding occurs subsequently by formation of additional hydrogen bonds closing the hairpin in the direction of the turn (zip-down mechanism). A second hairpin is formed at 15 ns, however, in a reverse manner: from the central turn toward the end (zip-up mechanism). The resulting 2:2 β-hairpin extends up to five residues on both sides of the turn (around 17.5 ns). A similar mechanism is observed in the 400 K left-handed helix simulation. Formation of the native β-turn in the last part (from 26 ns) of the 360 K extended conformation simulation occurs also by a zip-up mechanism. In all cases, the formation of backbone hydrogen bonds seems to be the initiating event for hairpin formation. Except for the first β-hairpin formation event at 12 ns in the α-helix simulation, which proceeds by a zip-down mechanism, all other events follow a mechanism in which the turn is first formed, followed by backbone hydrogen bond propagation. Once formed, these turns are stabilized by hydrophobic interactions, both in the native and C terminus shifted β-hairpins: hydrophobic contacts between Trp9, Arg10 and, to a lesser extent, Tyr11 stabilize the type I′ β-turn centred at Trp9, Arg10 in the native hairpin, while interactions between Trp9 and Tyr11 stabilize the type II′ β-turn at Tyr11-Ser12 in the shifted hairpin. The appearance of hydrophobic clusters stabilizing the turn conformations follows β-turn and hairpin formation. This mechanism is thus consistent with the zip-up model of Muñoz *et al*. (1997, 1998). One should however avoid generalizing these results, since various peptide sequences might lead to different mechanisms. In the C-terminal hairpin of protein G, hydrophobic residues are found in the middle of the hairpin while in tendamistat (this work) they are mainly located around the turn. This difference could explain the different β-hairpin formation mechanisms observed for the tendamistat β-hairpin (zip-up) (this work) and the protein G β-hairpin (zip-down) (Pande & Rokhsar, 1999; Dinner *et al*., 1999). In the 360 K extended conformation simulation, formation of an hydrophobic cluster following the initial collapse is observed, but, as was stated before, works against the formation of the native hairpin: this cluster has first to be disrupted and the structure turned inside-out to allow for β-hairpin formation.

Can we identify native-like conformations?

The results presented above have been described in terms of secondary structure content as a function of time and have been used to analyse the various trajectories. From these it is easy to identify ''folded'' structures with well-defined conformations such as β-hairpins or α-helices. Some of these have native characteristics, some do not. Can we find criteria that will allow us to unequivocally identify native-like conformations? To date, such criteria have remained elusive. In some studies a correlation could be demonstrated between terms such as hydrogen-bonding energies or contact areas and native structure, for example, in the refolding simulations of a β-hairpin from barnase (Prévost & Ortmans, 1997). This was, however, only possible by considering *a priori* knowledge of the native structure. Without any knowledge of which interactions or subset of interactions to monitor, identifying native-like or folded conformations from energetic (enthalpic) considerations remains extremely difficult, if possible. In our system for example, considering the oxidized and reduced 400 K simulations (Figure 1(a) and (b)), no significant difference in energies, solvent-accessible areas or number of hydrogen bonds (Table 1)

could be found to account for the difference in stability of the two systems. Similarly, if we only consider stable or native-like conformations within one simulation, as in for example the 2:2 β-hairpin present between 15, ns and 17.5 ns in the 400 K α-helix simulation, or the native-like β-turn conformations sampled in the last 4 ns of the 360 K simulation, again none of the above mentioned criteria can distinguish them from the remaining conformations sampled in those simulations (Table 2). In a more systematic approach, the backbone atom positional rms deviations from the native β-hairpin for the central eight residues were used to test the ability of the various quantities listed in Tables 1 and 2 to identify native-like conformations. Results in terms of correlation coefficients (R) for the 400 K (all reduced peptide 400 K simulations) and 360 K simulations are listed in Table 3. No significant correlation could be found between any energetic term and the deviation from the native β-hairpin. The highest of ''correlation'' ($R = 0.36$) is obtained for the internal van der Waals energy. This is also reflected in the correlation coefficients for solvent-accessible surface area (ASA): the highest correlation for the 360 K data is found for the ASA of non-polar atoms with $R = 0.46$. If only the central eight residues are considered, the correlation coefficients (given between parentheses in Table 3) increase to values of around 0.5, which is still of little use for identifying native-like conformations. The best correlation is obtained for the radius of gyration (R_g), which is not surprising since β-hairpin conformations are quite extended and therefore have larger R_g values than other unfolded conformations. In particular, if only the central eight hairpin residues are considered, a correlation coefficient of 0.95 for the radius of gyration against the atom-positional rmsd from the native form is obtained for the 360 K simulation. When α-helical conformations are sampled, as in the 400 K simulations, the correlation coefficient drops again to values of around 0.5. This indicates that, in this particular case, the radius of gyration cannot properly distinguish hairpin conformations from helical conformations. Similar results are obtained when using the atom-positional rms deviations from the average 300 K β-hairpin conformation for the linear fitting (data not shown). Multiple linear regressions using any combination of the terms listed in Table 3 only result in marginal improvements of the correlation coefficients. These results indicate that neither energetic (enthalpic) quantities nor geometric descriptors such as solvent accessible surface areas of particular types of atoms are suitable indicators of folded, native-like conformation.

Re-inspecting the data in Table 2 reveals a consistent trend, not in the averages (first moments), but in the fluctuations (second moments): a reduction in fluctuations of the energetic and solvent-accessible surface area terms is observed in the parts of the trajectories corresponding to folded structures. This can be clearly seen in the 400 K simulation when the 2:2 β-hairpin is formed (between 15.5 and 17.5 ns). From thermodynamics, enthalpy fluctuations can be related to the heat

Table 2. Average energies and structural characteristics from the folding MD simulations of the reduced peptide

	α-helix 400 K		Extended 360 K	
	0-29.5 ns	15.5-17.5 ns	0-30 ns	26.5-28.5 ns
A. *Energies (kJ mol^{-1})*				
E_{bonded} (solute)	689(13)	688(16)	634(17)	641(18)
E_{elec1} (solute-solute)	−487(79)	−565(67)	−465(74)	−466(68)
E_{elec2} (solute-solvent)	−1462(151)	−1324(124)	−1570(139)	−1578(130)
E_{elec} ($E_{elec1} + E_{elec2}$)	−1949(75)	−1889(59)	−2035(70)	−2044(65)
E_{vdw1} (solute-solute)	−421(33)	−414(21)	−443(31)	−446(29)
E_{vdw2} (solute-solvent)	−320(25)	−330(14)	−336(21)	−335(23)
E_{vdw} ($E_{vdw1} + E_{vdw2}$)	−741(17)	−744(16)	−779(20)	−781(15)
$E_{non\text{-}bonded}$ ($E_{elec} + E_{vdw}$)	−2690(71)	−2633(56)	−2814(65)	−2825(62)
B. *Solvent-accessible surface area (nm^2)*				
All atoms	18.8(1.4)	18.9(0.8)	18.1(1.3)	18.0(1.1)
Polar atoms	10.9(1.0)	11.3(0.6)	10.5(0.8)	10.6(0.8)
Non-polar atoms	7.9(0.8)	7.6(0.6)	7.7(0.8)	7.4(0.7)
Backbone	3.4(0.5)	3.2(0.4)	3.2(0.5)	3.1(0.4)
Side-chains	15.4(1.1)	15.6(0.7)	15.0(1.1)	14.9(0.9)
$R_{gyration}$ (backbone) (nm)	0.72(0.06)	0.75(0.07)	0.65(0.008)	0.64(0.05)
Number of hydrogen bonds	8.5(2.6)	8.8(2.3)	7.7(2.2)	8.4(2.1)
α-Helix (%)	6(1)	0(0)	0(2)	0(0)
β-Sheet (%)	4(1)	18(15)	5(10)	9(12)
β-Bridge (%)	4(6)	3(5)	4(6)	8(8)
β-Turn (%)	11(10)	11(6)	11(10)	11(10)
bend (%)	22(13)	23(12)	30(12)	31(10)

See legend to Table 1 for details.

Table 3. Correlation coefficients from a linear fit of various energetic and structural quantities against the backbone atom positional rms deviations from the native β-hairpin structure

	Reduced 400 K[a]	Reduced 360 K
A. *Energies (kJ mol^{-1})*		
E_{elec1} (solute-solute)	−0.14	0.12
E_{elec2} (solute-solvent)	0.15	−0.10
E_{elec} ($E_{elec1} + E_{elec2}$)	0.14	−0.06
E_{vdw1} (solute-solute)	0.15	0.36
E_{vdw2} (solute-solvent)	−0.05	−0.18
E_{vdw} ($E_{vdw1} + E_{vdw2}$)	0.20	0.36
$E_{non\text{-}bonded}$ ($E_{elec} + E_{vdw}$)	0.20	0.04
B. *Solvent-accessible surface area (nm^2)*		
All atoms	0.11(0.35)	0.39(0.55)
Polar atoms	0.18(0.35)	0.16(0.45)
Non-polar atoms	−0.02(0.21)	0.46(0.52)
Backbone	0.18(0.01)	0.38(0.49)
Side-chains	−0.09(0.40)	0.29(0.47)
$R_{gyration}$ (backbone)(nm)	0.10(0.54)	0.55(0.95)
Number of hydrogen bonds	−0.03(−0.03)	−0.27(−0.21)

The atom-positional rms deviations from the native β-hairpin structure used in the fitting were calculated for N, C^{α} and C-atoms of the central eight residues (6-13). The values between brackets correspond to correlation coefficients obtained from properties calculated only from the central eight residues (6-13).

[a] Structural data from all 400 K MD simulations (starting from native, α and left-handed helices) of the reduced peptide were used in the linear regressions.

capacity C_p. In particular, the transition excess heat capacity $\langle \Delta C_{p,tr} \rangle$, which measures the enhancement of enthalpic fluctuations associated with a conformational transition, can be written as (Freire, 1995):

$$\langle \Delta C_{p,tr} \rangle = (\langle \Delta H^2 \rangle - \langle \Delta H \rangle^2)/RT^2 = \sigma^2_{\Delta H}/RT^2$$

Changes in heat capacity can be monitored experimentally from calorimetry measurements. The method has been applied to the study of protein folding and the resulting heat capacity changes interpreted in terms of folding transitions (for a review, see Freire, 1995). This led us to investigate the energy fluctuations of the simulated peptide as a function of time. Energy fluctuations σ_E calculated over 1 ns periods for the sum of solute-solute and solute-solvent interactions for the 360 K simulation are displayed in Figure 5. One can clearly see that the energy fluctuations are not constant over time, a number of distinct peaks being present. Apart from the initial decrease, which can be attributed both to the higher simulation temperature at the beginning (400 K) (see Computational Methods) and the initial collapse from the extended conformation, two large peaks are present at 5 ns and 27 ns, respectively. The increased energy fluctuations around 5 ns precede the formation of a tight β-turn at Gln13-Ala14 and of an antiparallel β-sheet, as can be seen from Figure 2(c), and mark the disappearance of the initial conformational cluster, as can be seen from Figure 4. This increase in energy fluctuation is thus consistent with the formation of a more compact and ordered structure with some β-hairpin characteristics. Subsequently, σ_E decreases to reach a minimum of around 13 ns where a parallel β-sheet is present (Figures 2(c)) and 3(e)). The structural rearrangements around 16 ns leading to the formation of β-hairpin structures in the C-terminal part of the peptide are also accompanied by an increase in enthalpic fluctuation. This corresponds in the rmsd matrix shown in Figure 4 to the transition to a new conformational cluster around 16 ns. The appearance at 26 ns of the last conformational cluster which shows native-like characteristics, as indicated by the cross-peaks (lower right of the rmsd matrix) with the native 300 K and 400 K structures, is again accompanied by a large increase in energy fluctuations. The corresponding structures contain native like β-hairpin conformations with a type I β-turn at Trp9-Arg10 (Figures 2(c) and 3(e)). The observation that an increase of energy fluctuation accompanies conformational transitions is consistent with variations in heat capacity measured experimentally for protein folding. Monitoring such fluctuations in simulations can thus point to interesting parts of the MD trajectories where significant conformational rearrangements take place, but still does not allow to distinguish native-like conformations from others. These fluctuations should be calculated from sufficiently long portions of the MD trajectories to minimize the noise. Long MD simulations in the 10 ns to 100 ns time range are therefore required.

Conclusions

By comparing molecular dynamics simulations of the reduced and oxidized native peptides, the conservation of the disulphide bridge closing the β-hairpin among the family of α-amylase inhibitor could be rationalized through its role in maintaining a proper turn conformation, insuring thereby proper side-chains arrangements in the conserved turn residues. Removal of this bridge allows the

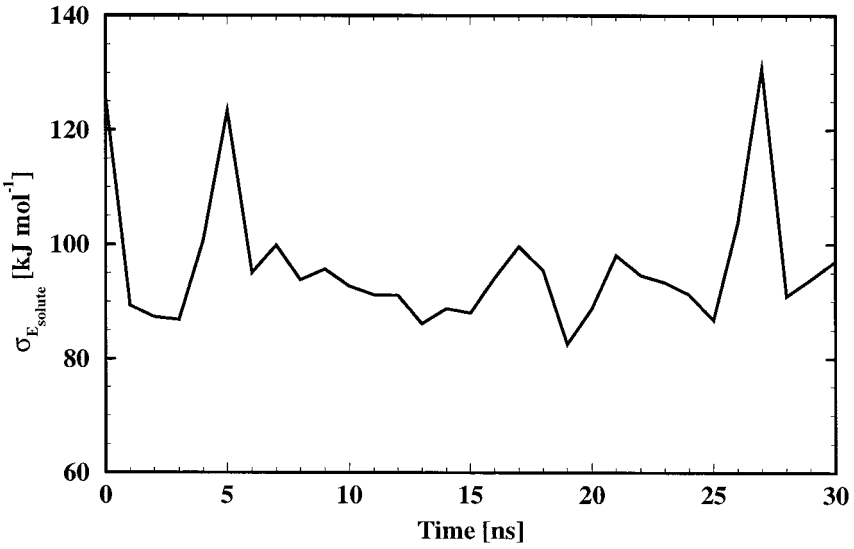

Figure 5. Peptide energetic fluctuations as a function of time for the 360 K MD simulation in water starting from the extended conformation. The fluctuations were calculated for the sum of solute-solute and solute-solvent energy terms over 1 ns time windows.

formation of non-native β-turns and shifted β-hairpin conformations that have also been identified from NMR measurement on a shorter peptide lacking the disulphide bridge (Blanco *et al.*, 1991). In high temperature folding simulations starting from different conformations, both native and non-native β-hairpin conformations were recovered. These remained stable for several nanoseconds before the system started sampling other regions of conformational space. Reducing the simulation temperature should perhaps allow us to quench or increase the occurrence of such conformations, at the cost of increasing simulation time since the rate of sampling conformational space will be reduced. The folding events monitored in the various simulations support a model for β-hairpin formation in which the turn is formed first, followed by hydrogen bond formation in a zip-up model. The hairpin, and in particular the β-turn, are subsequently stabilized by side-chain hydrophobic interactions. This mechanism however need not be universal, a hydrophobic collapse model having also been observed for different peptide sequences, for example for the C-terminal β-hairpin of protein G (Pande & Rokhsar, 1999; Dinner *et al.*, 1999). Both mechanisms have been proposed as early events in protein folding.

Although molecular dynamics simulations in explicit solvent remain expensive and reversible folding simulations in aqueous media have yet to be reported, simulating the folding process of short peptides at atomic detail is becoming feasible. Such simulations give a dynamic picture of peptide structure and lead to a better understanding of early events in protein folding. As demonstrated here, simulations starting from completely different initial configurations start sampling similar regions of the conformational space at high temperatures within tens of nanoseconds, indicating that only a limited portion of the accessible conformational space needs to be sampled. This is particularly encouraging, since no simple criteria could yet be identified to unequivocally distinguish native conformations from others. Without any *a priori* knowledge of the native structure, only sufficiently long molecular dynamics simulations or extensive sampling methods generating ensembles of conformations in an equilibrium distribution will allow the prediction of native-like structures. This has been demonstrated recently from molecular dynamics simulations of β-peptides (Daura *et al.*, 1998a, 1999) in methanol and for short natural peptides using an implicit solvent model and biased molecular dynamics (Schaefer *et al.*, 1998). Considering the continuous improvements in hardware, empirical force fields and simulation techniques, a reliable description of peptide folding and structure based on simulations is within reach. For proteins, however, although a milestone has been set by a 1 μs simulation of a small protein in water (Duan & Kollman, 1998), equilibrium simulations of protein dynamics and folding will still remain inaccessible for the near future.

Computational Methods

Molecular model and interactions

The peptide and water were modelled according to the GROMOS96 model and force field 43A1 (van Gunsteren *et al.*, 1996; Daura *et al.*, 1998b).

System setup

The initial structure of the 19-residue peptide sequence, SCVTLYQSWRYSQADNGCA, corresponding to the first β-hairpin (residues 10 to 28) of the α-amylase inhibitor tendamistat was taken from the NMR structure (PDB entry 3AIT) (Billeter *et al.*, 1990). The reduced and oxidized forms were first energy-minimised and then solvated in a periodic truncated octahedron box of single point charge (SPC) water (Berendsen *et al.*, 1981) with a

minimum solute-wall distance of 1.0 nm. The two systems were subsequently submitted to two times 250 steps of steepest descent energy minimization to remove bad contacts between the peptide and the water. The peptide coordinates were fixed in the first minimization and position restraints with force constants of 5000 kJ mol^{-1} nm^{-2} were applied in the second minimization. The final systems comprised 202/204 solute atoms and 2441/2440 water molecules, amounting to a total of 7525 and 7524 atoms for the oxidized and reduced forms, respectively.

The α and left-handed helical structures and the extended structure of the reduced form used in the folding runs were built with Macromodel (Mohamadi *et al.*, 1990) and subjected to the same protocol as the native reduced form taken from the NMR structure. For the two helical conformations, the box size was chosen such as to obtain the same number of water molecules as for the native form, resulting in minimum solute-wall distances of 1.105 and 1.13 nm, respectively. For the extended form, the initial system comprised 6718 water molecules. Because of the fast collapse of the extended conformation, the amount of water molecules in the system could be reduced twice, after 0.2 ns and 0.4 ns of molecular dynamics simulation at 400 K, respectively, resulting in the same number of water molecules (2440, minimum solute wall distance of 1.33 nm) as for the native reduced form. This conformation was used as starting point for the 360 K MD simulation.

MD simulation

The simulations were run for variable time periods, ranging from 10 to 30 ns using the GROMOS96 MD program (van Gunsteren *et al.*, 1996, Scott *et al.*, 1999). The time-step used in the leap-frog integration scheme was 0.002 ps. Covalent bond lengths were constrained with the procedure SHAKE (Ryckaert *et al.*, 1977) with a relative geometric tolerance of 0.0001. The initial velocities were taken from a Maxwellian distribution at the chosen temperature (300, 360 or 400 K). The temperature of the system was maintained by weakly coupling solute and solvent, separately, to an external temperature bath at the reference temperature (Berendsen *et al.*, 1984). The temperature coupling constant was 0.1 ps (0.01 in the first 50 ps). The pressure was maintained by weakly coupling the system to an external pressure bath at one atmosphere with a coupling constant of 0.5 ps (0.05 during the first 50 ps). The non-bonded interaction pair list was updated every five steps with a cut-off of 0.8 nm. The non-bonded interactions were calculated with group cut-offs using the twin-range method (van Gunsteren & Berendsen, 1990) with cut-offs of 0.8 and 1.4 nm, respectively: all non-bonded interactions within 0.8 nm were calculated at every step, while the long-range contribution, up to 1.4 nm, was updated every five steps. A reaction field correction (Tironi *et al.*, 1995) was used with a permittivity ε_{RF} of 54, which corresponds to the dielectric permittivity calculated for the SPC water model (Smith & van Gunsteren, 1994). Position restraints were applied on the solute heavy atoms during the first 40 ps of the simulations, with decreasing force constants of 5000, 500, 50 and 5 kJ mol^{-1} nm^{-2}, respectively, to allow the water to equilibrate without disturbing the peptide structure. Coordinates were saved every 0.5 ps for analysis.

The simulations were performed on a variety of SGI systems, using both serial and shared-memory parallel versions of GROMOS96. As a CPU cost indication, 1 ns trajectory required 5 CPU days on a single SGI R10000 195 MHz processor.

Secondary structure analysis

The secondary structure content of the peptides was calculated using the SECSTR module of the program PROCHECK (Laskowski *et al.*, 1993).

Solvent-accessible surface area

Solvent accessible surface area was calculated with the program NACCESS (Hubbard & Thornton, 1993), using a 0.14 nm radius probe.

Acknowledgements

The authors thank Drs Alan Mark and Xavier Daura (ETH Zürich) for numerous helpful discussions and Dr Rainer Wechselberger (Utrecht University) for careful reading of the manuscript. Financial support was obtained from the Schweizerischer Nationalfonds, project number 21-050929.97, which is gratefully acknowledged.

References

Berendsen, H. J. C., Postma, J. P. M., van Gunsteren, W. F. & Hermans, J. (1981). Interaction models for water in relation to protein hydration. In *Intermolecular Forces* (Pullman, B., ed.), pp. 331-342, , Dordrecht, Reidel.

Berendsen, H. J. C., Postma, J. P. M., van Gunsteren, W. F., DiNola, A. & Haak, J. R. (1984). Molecular dynamics with coupling to an external bath. *J. Chem. Phys.* **81**, 3684-3690.

Billeter, M., Schaumann, T., Braun, W. & Wüthrich, K. (1990). Restrained energy refinement with two different algorithms and force fields of the structure of the α-amylase inhibitor tendamistat determined by NMR in solution. *Biopolymers*, **29**, 695-724.

Blanco, F. J., Jiménez, M. A., Rico, M., Santoro, J., Herranz, J. & Nieto, J. L. (1991). Tendamistat (12-26) fragment. NMR characterization of isolated β-turn intermediates. *Eur. J. Biochem.* **200**, 345-351.

Blanco, F. J., Rivas, G. & Serrano, L. (1994). A short linear peptide that folds into a β-hairpin in aqueous solution. *Nature Struct. Biol.* **1**, 584-590.

Blanco, F. J., Ramirez-Alvarado, M. & Serrano, L. (1998). Formation and stability of β-hairpin structures in polypeptides. *Curr. Opin. Struct. Biol.* **8**, 107-111.

Chan, H. S. & Dill, K. A. (1998). Protein folding in the landscape perspective: chevron plots and non-Arrhenius kinetics. *Proteins: Struct. Funct. Genet.* **30**, 2-33.

Daura, X., Jaun, B., Seebach, D., van Gunsteren, W. F. & Mark, A. E. (1998a). Reversible peptide folding in solution by molecular dynamics simulations. *J. Mol. Biol.* **280**, 925-932.

Daura, X., Mark, A. E. & van Gunsteren, W. F. (1998b). Parameterization of the aliphatic CH_n united atoms of the GROMOS96 force field. *J. Comp. Chem.* **19**, 535-547.

Daura, X., van Gunsteren, W. F. & Mark, A. E. (1999). Folding-unfolding thermodynamics of a beta-hepta-

peptide from equilibrium simulations. *Proteins: Struct. Funct. Genet.* **34**, 269-280.
de Alba, E., Jiménez, M. A., Rico, M. & Nieto, J. L. (1996). Conformational investigation of designed short linear peptides able to fold into β-hairpin structures in aqueous solution. *Fold. Design,* **1**, 133-144.
de Alba, E., Santoro, J., Rico, M. & Jiménez, M. A. (1999). *De novo* design of a monomeric three-stranded antiparallel β-sheet. *Protein Sci.* **8**, 854-865.
Demchuk, E., Bashford, D. & Case, D. (1997). Dynamics of a type VI turn in a linear peptide in aqueous solution. *Fold. Design,* **2**, 35-46.
Dinner, A. R., Sali, A. & Karplus, M. (1996). The folding mechanism of larger model proteins: role of native structure. *Proc. Natl Acad. Sci. USA,* **93**, 8356-8361.
Dinner, A. R., Lazaridis, T. & Karplus, M. (1999). Understanding β-hairpin formation. *Proc. Natl Acad. Sci. USA,* **96**, 9068-9073.
Dobson, C. M. & Karplus, M. (1999). The fundamental of protein folding: bringing together theory and experiment. *Curr. Opin. Struct. Biol.* **9**, 92-101.
Duan, Y. & Kollman, P. A. (1998). Pathways to a protein-folding intermediate observed in a 1-microsecond simulation in aqueous solution. *Science,* **282**, 740-744.
Fisher, D. & Eisenberg, D. (1999). Predicting structures for genome proteins. *Curr. Opin. Struct. Biol.* **9**, 208-211.
Freire, E. (1995). Thermal denaturation methods in the study of protein folding. *Methods Enzymol.* **259**, 144-168.
Gellman, S. H. (1998). Minimal model systems for beta sheet secondary structure in proteins. *Curr. Opin. Chem. Biol.* **2**, 717-725.
Gutin, A. M., Abkevich, V. I. & Shaklnnovich, E. I. (1995). Is burst hydrophobic collapse necessary for protein folding? *Biochemistry,* **34**, 3066-3076.
Hubbard, S. J. & Thornton, J. M. (1993). *''NACCESS'' Computer Program*, Department of Biochemistry and Molecular Biology, University College London.
Kortemme, T., Ramirez-Alvarado, M. & Serrano, L. (1998). Design of a 20-amino acid, three-stranded beta-sheet protein. *Science,* **281**, 253-256.
Kraulis, P. J. (1991). MOLSCRIPT: a program to produce both detailed and schematic plots of protein structures. *J. Appl. Crystallog.* **24**, 946-950.
Lacroix, E., Kortemme, T., Lopez de la Paz, M. & Serrano, L. (1999). The design of linear peptides that fold as monomeric β-sheet structures. *Curr. Opin. Struct. Biol.* **9**, 487-493.
Laskowski, R. A., MacArthur, M. W. & Thornton, J. M. (1993). PROCHECK: a program to check the stereochemical quality of protein structures. *J. Appl. Crystallog.* **26**, 283-291.
Merritt, E. A. & Murphy, M. E. P. (1994). Raster3D version 2.0, a program for photorealistic molecular graphics. *Acta Crystallog. sect. D,* **50**, 869-873.
Mirny, L. A., Abkevich, V. & Shakhnovich, E. I. (1996). Universality and diversity of the protein folding scenarios: a comprehensive analysis with the aid of lattice model. *Fold. Design,* **1**, 103-116.
Mohamadi, F., Richards, N. G. J., Guida, W. C., Liskamp, R., Lipton, M., Caufield, C., Chang, G., Hendrickson, T. & Still, W. C. (1990). MacroModel-an integrated soft-ware system for modeling organic and bioorganic molecules using molecular mechanics. *J. Comp. Chem.* **11**, 440-467.
Muñoz, V., Thompson, P. A., Hofrichter, J. & Eaton, W. (1997). Folding dynamics and mechanism of β-hairpin formation. *Nature,* **390**, 196-199.
Mũnoz, V., Henry, E. R., Hofrichter, J. & Eaton, W. (1998). A statistical mechanical model for β-hairpin kinetics. *Proc. Natl Acad. Sci. USA,* **95**, 5872-5879.
Pande, V. S., Grosberg, A. Y., Tanaka, T. & Rokhsar, D. S. (1998). Pathways for protein folding: is a new view needed? *Curr. Opin. Struct. Biol.* **8**, 68-79.
Pande, V. S. & Rokhsar, D. S. (1999). Molecular dynamics simulations of unfolding and refolding of a β-hairpin fragment of protein G. *Proc. Natl Acad. Sci. USA,* **96**, 9062-9067.
Prévost, M. & Ortmans, I. (1997). Refolding simulations of an isolated fragment of barnase into a native-like β hairpin: evidence for compactness and hydrogen bonding as concurrent stabilizing factors. *Proteins: Struct. Funct. Genet.* **29**, 212-227.
Ramachandran, G. N., Ramakrishnan, C. & Sasisekharan, V. (1963). Stereochemistry of polypeptide chain configurations. *J. Mol. Biol.* **7**, 95-99.
Ramirez-Alvarado, M., Blanco, F. J. & Serrano, L. (1996). *De novo* design and structural analysis of a model β-hairpin peptide system. *Nature Struct. Biol.* **3**, 604-611.
Reagan, L. (1999). Protein redesign. *Curr. Opin. Struct. Biol.* **9**, 494-499.
Ryckaert, J.-P., Ciccotti, G. & Berendsen, H. J. C. (1977). Numerical integration of the Cartesian equations of motion of a system with constraints: molecular dynamics of *n*-alkanes. *J. Comp. Phys.* **23**, 327-341.
Schaefer, M., Bartels, C. & Karplus, M. (1998). Solution conformations and thermodynamics of structured peptides: molecular dynamics simulation with an implicit solvation model. *J. Mol. Biol.* **284**, 835-848.
Schönbrunner, N., Wey, J., Engels, J., Georg, H. & Kiefhaber, T. (1996). Native-like β-structure in a trifluoroethanol-induced partially folded state of the all-β-sheet protein tendamistat. *J. Mol. Biol.* **260**, 432-445.
Schönbrunner, N., Koller, K.-P. & Kiefhaber, T. (1997a). Folding of the disulphide-bonded β-sheet protein tendamistat: rapid two-state folding without hydrophobic collapse. *J. Mol. Biol.* **268**, 526-538.
Schönbrunner, N., Pappenberger, G., Scharf, M., Engels, J. & Kiefhaber, T. (1997b). Effect of preformed correct tertiary interactions in rapid two-state tendamistat folding: evidence for hairpins as initiation sites for β-sheet formation. *Biochemistry,* **36**, 9057-9065.
Scott, W. R. P., Hünenberger, P. H., Tironi, I. G., Mark, A. E., Billeter, S. R., Fennen, J., Torda, A. E., Huber, T., Krüger, P. & van Gunsteren, W. F. (1999). The GROMOS biomolecular simulation program package. *J. Phys. Chem. A,* **103**, 3596-3607.
Scully, J. & Hermans, J. (1994). Backbone flexibility and stability of reverse turn conformation in a model system. *J. Mol. Biol.* **235**, 682-694.
Searle, M. S., Williams, D. H. & Packman, L. C. (1995). A short linear peptide derived from the N-terminal sequence of ubiquitin folds into a water-stable non-native β-hairpin. *Nature Struct. Biol.* **2**, 299-1006.
Shakhnovich, E. I. (1997). Theoretical studies of protein-folding thermodynamics and kinetics. *Curr. Opin. Struct. Biol.* **7**, 29-40.
Sibanda, B. L. & Thornton, J. M. (1984). β-hairpin families in globular proteins. *Nature,* **316**, 170-174.
Sieber, V. & Moe, G. R. (1996). Interactions contributing to the formation of a β-hairpin-like structure in a small peptide. *Biochemistry,* **35**, 181-188.

Smith, P. E. & van Gunsteren, W. F. (1994). Consistent dielectric properties of the simple point charge and extended simple point charge water models at 277 and 300 K. *J. Chem. Phys.* **100**, 3169-3174.

Socci, N. D., Onuchic, J. N. & Wolynes, P. G. (1998). Protein folding mechanisms and the multidimensional folding funnel. *Proteins: Struct. Funct. Genet.* **32**, 136-158.

Thirumalai, D. & Klimov, D. K. (1999). Deciphering the timescales and mechanisms of protein folding using minimal off-lattice models. *Curr. Opin. Struct. Biol.* **9**, 197-207.

Tironi, I. G., Sperb, R., Smith, P. E. & van Gunsteren, W. F. (1995). A generalized reaction field method for molecular dynamics simulations. *J. Chem. Phys.* **102**, 5451-5459.

Tobias, D. J., Mertz, J. E. & Brooks, C. L., III (1991). Nanosecond time scale folding dynamics of a pentapeptide in water. *Biochemistry,* **30**, 6054-6058.

van Gunsteren, W. F. & Berendsen, H. J. C. (1990). Computer simulation of molecular dynamics: methodology, applications and perspectives in chemistry. *Angew. Chem. Int. Edit.* **29**, 992-1023.

van Gunsteren, W. F., Billeter, S. R., Eising, A. A., Hünenberger, P. H., Krüger, P., Mark, A. E., Scott, W. R. P. & Tironi, I. G. (1996). *Biomolecular Simulation: The GROMOS96 Manual and User Guide*, pp. 1-1042, Vdf Hochschulverlag AG an der ETH Zurich, Zürich, Switzerland.

Edited by A. R. Fersht

(Received 16 September 1999; received in revised form 9 December 1999; accepted 9 December 1999)